Journal of Physics D:
Applied Physics

PAPER

InGaN-based light-emitting diodes with thyristor characteristic

To cite this article: Ping Chieh Tsai *et al* 2025 *J. Phys. D: Appl. Phys.* **58** 205101

IOP Publishing

Journal of Physics D: Applied Physics

J. Phys. D: Appl. Phys. 58 (2025) 205101 (9pp)

https://doi.org/10.1088/1361-6463/adc8b4

InGaN-based light-emitting diodes with thyristor characteristic

Ping Chieh Tsai[1], **Chunyu Zhao**[1], **Swee Tiam Tan**[2,*] **and Hilmi Volkan Demir**[1,3,4,*]

[1] LUMINOUS! Center of Excellence for Semiconductor Lighting and Displays, School of Electrical and Electronic Engineering, Nanyang Technological University, 50 Nanyang Avenue, Singapore 639798, Singapore
[2] Kelip-kelip! Center of Excellence for Light Enabling Technologies, School of Energy and Chemical Engineering, Xiamen University Malaysia, Daerah Sepang, Selangor Darul Ehsan 43900, Malaysia
[3] School of Physics and Mathematical Sciences, Division of Physics and Applied Physics, Nanyang Technological University, 21 Nanyang Link, Singapore 637371, Singapore
[4] Department of Electrical and Electronics, Department of Physics, and National Nanotechnology Research Center Institute of Material Science and Nanotechnology, Bilkent University, Ankara TR-06800, Turkey

E-mail: sweetiam.tan@xmu.edu.my and hvdemir@ntu.edu.sg

Received 5 November 2024, revised 5 March 2025
Accepted for publication 2 April 2025
Published 22 April 2025

Abstract

We propose and demonstrate the InGaN-based light-emitting diodes (LEDs) with thyristor function for the first time by incorporating an Mg-doped *p*-GaN layer between the *n*-GaN layer and InGaN/GaN multiple-quantum-well active layer. Utilizing the thyristor-like structure, a distinctive negative differential resistance (NDR) appears on the *I*–*V* characteristics of InGaN-based LEDs. This unique bi-switching characteristics of the thyristor will enable a fast switching of the LEDs and thus reducing the complexity of the driving circuit design, making it a potential switching devices in the field of optical communications. In this work, the Mg doping concentration and thickness of the additionally added *p*-GaN layer were found to have a significant impact on the NDR. The formation of NDR becomes more and more obvious with the increase of Mg doping and thickness. In our structure, the Mg doping flow rate of about 0.583–1.057 μmol min^{-1} and the thickness of about 300–400 nm yield the best NDR properties. The brightness of LEDs decreases monotonically with the increasing Mg doping flow rate. Moreover, when the Mg doping concentration is insufficient, two NDR regions will appear in the *I*–*V* characteristics as the thickness increases. When the thickness is set to 300 nm and the Mg doping flow rates are 0.583, 0.802, and 1.057 μmol min^{-1}, the optical output powers of the LEDs are measured to be 13.1, 12.8, and 14.3 mW at the driving current of 201 mA while the output powers at 4.61 mA are 0.46, 0.52, and 0.54 mW. The forward voltages at 201 mA are 3.71, 3.75, and 3.95 V for the Mg doping flow rates of 0.583, 0.802, and 1.057 μmol min^{-1}, respectively. The characteristics of the thyristor-like InGaN LEDs need to be further optimized to reduce the operating current.

Keywords: GaN, light-emitting diode (LED), thyristor, negative differential resistance (NDR)

* Authors to whom any correspondence should be addressed.

1. Introduction

In the past decades, InGaN-based III–V semiconductor light-emitting diodes (LEDs) have emerged as important candidate in the solid-state lighting and display industry due to their low power consumption, long operation life, high luminescence efficiency, being mercury-free, and extensive spectra coverage from ultraviolet to near-infrared [1–3]. In these applications, LEDs usually serve as a light source that require a controller to control its on and off mode. Hence, the bipolar junction transistor or the field-effect transistor is usually deployed as a controller for the LED devices. However, such a design will lead to an increase in complexity of the LED driver circuit, especially in the advanced application such as compact liquid crystal display, or micro or mini LED display [4, 5]. The quantity of transistors will significantly increase the complexity in circuit design as well as fabrication.

On the other hand, optical devices with fast switching functions are well-suited for use in optical interconnections and mobile communication such as light fidelity (LiFi) [6], and parallel optical information processing [7]. Some structures such as vertical-to-surface transmission electrophotonic devices [8] or double heterostructure optoelectronic switches (DOES) [9] have been proposed for optical interconnection or communication applications. In particular, depleted optical thyristor (DOT) based on the DOES concept has been demonstrated [10]. To achieve fast bistable switching speed, the DOT structure is a good candidate for data communication. It exhibits excellent response since it can be completely depleted by reverse biasing the *p*–*n* junction, and the excess carriers in the active layer can be expelled in less than tens of picoseconds. However, most of these studies focus on GaAs-based or InP-based material systems. To our best knowledge, very little research has been done on GaN-based materials.

The thyristor architecture is composed of a four-layer p_2–n_2–p_1–n_1 junction [11]. It is a bistable device that possesses high impedance, low current in the OFF-state, and low impedance, high current in the ON-state. By combining this distinctive bistable characteristic with the LED, one can expect the LED can be switched from the OFF-state, which does not emit light, to the ON-state, which emits light, via a proper applied voltage. To achieve this purpose, an extra *p*-GaN layer is introduced into the regular GaN-based LED structure between the *n*-GaN and the multiple-quantum-well (MQW) in our study. With this device architecture, we could extend the optical switching to shorter wavelengths, even to the ultraviolet band. In this way, we can realize LiFi application on the network of local areas, such as home or office, and many other applications that require LEDs with a switching function.

2. Experiments

The thyristor-like InGaN-based LEDs in this study were grown on a 2-inch *c*-plane (0001) patterned sapphire substrate using a metal–organic chemical vapor deposition system. For the growth of the III-N epilayers, trimethylgallium (TMGa), trimethylindium (TMIn), trimethylaluminum (TMAl), and ammonia (NH_3) were used as Ga, In, Al, and N sources, respectively. Silane (SiH_4) and bis-cyclopentadienyl magnesium (Cp_2Mg) were used as *n*-type and *p*-type dopants, respectively. The structure consists of a 30 nm-thick GaN nucleation layer grown at 550 °C, a 2 μm-thick undoped GaN epilayer grown at 1050 °C, a 3 μm-thick Si-doped GaN epilayer, a 30 nm-thick Si-doped AlGaN, a Si-doped $In_{0.12}Ga_{0.88}N$ strain relief layer (SRL) grown at 950 °C, an $In_{0.23}Ga_{0.77}N$/GaN MQW active layer grown at 800 °C, a 50 nm-thick Mg-doped AlGaN as the electron blocking layer (EBL), and finally a 195 nm-thick Mg-doped GaN epilayer grown at 1000 °C. The MQW active layer consists of eight periods of a 3 nm-thick undoped InGaN well layer and a 7 nm-thick Si-doped GaN barrier layer. Note that the Si doping concentration in the quantum barrier is much lower than that of the *n*-GaN layer. For the growth of thyristor-like InGaN-based LEDs, an additional *p*-GaN layer was introduced between the *n*-GaN and the MQW. To find the best epitaxy growth conditions, we enlarged the range of parameter settings in the experimental design. The Mg doping flow rate in this layer was 0.018–1.349 μmol min^{-1}, and the thickness was 50–900 nm. The parameters *a* and *b* of organometallic saturated vapor pressure can be referred to in [12]. Table 1 details the doping flow rate and thickness for each experiment. Due to improper experimental parameter settings causing abnormal *I*–*V* characteristics, to present our research results clearly and concisely, some parameters are not shown in our figures in the following analysis, but the overall trend is consistent. To distinguish the properties of each layer, we marked *n*-GaN and *n*-AlGaN as the n_1 layer, the additionally inserted *p*-GaN was named the p_1 layer, SRL, and MQW were designated as the n_2 layer, and finally, EBL and *p*-GaN were labeled the p_2 layer. The detailed structure is shown in figure 1. Figures 1(a)–(c) respectively show general InGaN-based LEDs, *p*–*n* type thyristors with 4 junctions ($p2$–$n2$–$p1$–$n1$), and InGaN-based LEDs with thyristor structures. In the epitaxial process, the doping profile of thyristor-like InGaN-based LEDs can be referred to [11].

Table 1. Experimental parameter settings for $p1$ layer.

Mg flow (μmol min^{-1})	$p1$ thickness (nm) 50	100	300	400	500	700	900
0.018			*				
0.036		*	*		*	*	*
0.073			*		*	*	*
0.146		*	*		*	*	*
0.255			*		*	*	*
0.401			*		*	*	
0.583		*	*	*			
0.802	*	*	*	*			
1.057	*	*	*				
1.349	*	*	*				

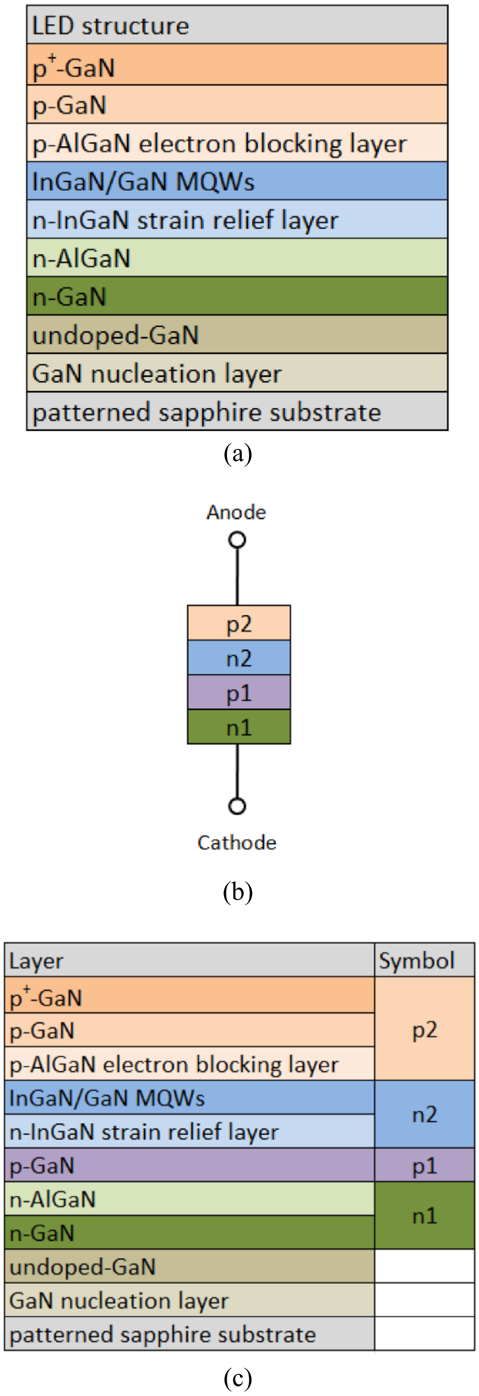

Figure 1. Schematic structures for (a) general InGaN-based LEDs, (b) *p*–*n* type thyristor with 4 junctions, and (c) thyristor-like InGaN-based LEDs.

After the growth, the *p*-GaN surface (p_2) of the as-grown sample was then partially etched until the *n*-GaN (n_1) layer was exposed. Next, indium tin oxide (ITO) was deposited on the *p*-GaN (p_2) surface as the transparent contact layer. Afterward, Ni–Au and Ti–Al–Ti–Au were deposited on *p*-GaN (p_2) and exposed *n*-GaN (n_1) surface as *p*- and *n*-type electrodes to complete the fabrication of LEDs, respectively. Finally, the chip size was cut into a rectangular shape of 760 μm $\times$ 640 μm for subsequent measurements. Next, the *I*–*V* characteristics test was executed using a Keithley 2400 source meter. The optical output power of LEDs was measured using the integrating sphere attached to an Ocean Optics spectrometer (QE65000) and Advantest R6243 DC voltage current source. To minimize Joule heating, a pulsed current with a width of 10 ms and a duty cycle of 20% was employed to measure the output power of the LED.

3. Results and discussion

Figure 2 shows the *I*–*V* characteristics of thyristor-like InGaN-based LEDs with $p1$ layer thicknesses of 100, 300, and 500 nm at Mg doping flow rates of 0.036–1.349 μmol min^{-1}. It can be found that the *I*–*V* characteristics with negative differential resistance (NDR) become more apparent with the increase of Mg doping flow rate. The forward breakover voltage (V_{BF}) also increases with the increase of the Mg doping flow rate and decreases upon the high flow rate (1.349 μmol min). It is worth noting that when the thickness of p_1 is too thick (900 nm), the LED will suffer from severe localized heating under high current injection, causing permanent damage to the devices (not shown here). As shown in figure 2(b), the *I*–*V* curve shifts to the right as the doping flow rate increases until the doping flow rate reaches 0.255 μmol min^{-1}. The *I*–*V* curve then shifts to the left when the doping flow rate is between 0.255 and 1.057 μmol min^{-1}. Finally, the *I*–*V* curve shifted to the right again at a very high doping flow rate of 1.349 μmol min^{-1}. Meanwhile, it can be found that their *I*–*V* characteristics are almost consistent when the Mg doping flow rates are between 0.583 and 1.057 μmol min^{-1}. Moreover, the holding voltage (V_{h}) is also lower than that at low Mg doping flow rates ($\leqslant$0.255 μmol min^{-1}) at the same current. For the Mg doping flow rates of 0.583, 0.802, and 1.057 μmol min^{-1}, the forward conduction voltage (V_{f}) at 201 mA is 3.71, 3.75, and 3.95 V, respectively. On the other hand, it can be found from figure 2 that when the thickness is too thick ($\geqslant$300 nm) or the Mg doping flow rate is too small ($\leqslant$0.255 μmol min^{-1}), two NDR regions will appear in the *I*–*V* characteristics, such as figures 2(b) and (c). The reasons for the formation of the two NDR regions will be discussed later.

Figure 3 shows the energy-band diagram to illustrate the change in the *I*–*V* characteristics [11]. To simplify the energy-band diagram, we represent the thyristor-like InGaN-based LEDs as a p_2–n_2–p_1–n_1 structure with three junctions. Figure 3(a) is the energy-band diagram of the p_1 layer with a low Mg doping flow rate at thermal equilibrium. The Fermi level (E_{F}) is further away from the valence band when the p_1 layer is at a low doping flow rate, such as 0.018–0.073 μmol min^{-1}. Compared with a low doping flow rate, the difference in the energy-band diagram at thermal equilibrium is that a high doping flow rate has a larger barrier height at junction 1 (Jp_1/n_1). When a positive potential is applied at the anode (p_2) for the cathode (n_1), the junction Jp_1/n_1 and Jp_2/n_2

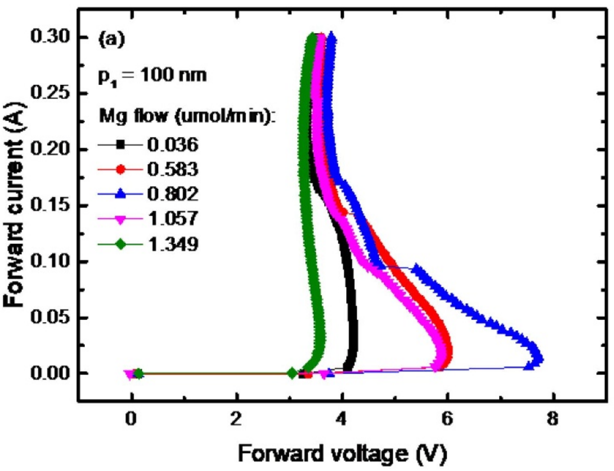

(a)

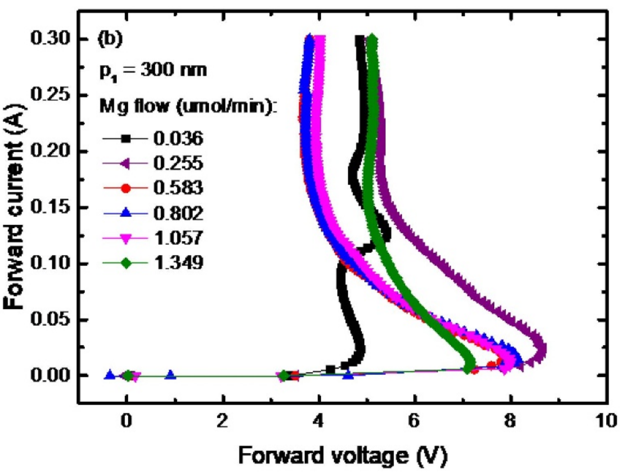

(b)

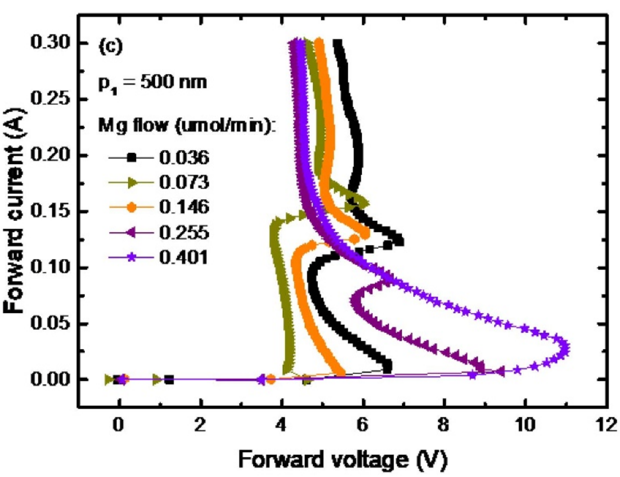

(c)

Figure 2. *I–V* characteristics of the thyristor-like InGaN-based LEDs with different Mg doping flow rates at thicknesses ranging from 100 to 500 nm.

are forward biased, while junction Jn_2/p_1 is reverse biased, as shown in figure 3(b). Note that the doping flow rate of n_2 among these four layers is the lowest. So the depletion region at Jn_2/p_1 becomes very wide due to low carrier concentration in the n_2 layer, resulting in the OFF-state for the LEDs. In this case, the *I–V* characteristics in the forward blocking region in figure 2 show a large voltage but a small current. Nevertheless, the voltage at this time is still lower than the V_{BF}. Once the applied voltage becomes large, the electrons from the n_1 layer start to cross Jp_1/n_1 after gaining enough energy. When the electrons enter the p_1 layer across Jp_1/n_1, the V_{BF} shown in figure 2 is formed. At this moment, compared with the high doping flow rate under the same injection current, the electrons in the n_1 layer are more likely to cross the energy barrier at Jp_1/n_1 and then enter the p_1 layer when the p_1 layer is low-doped. Therefore, the V_{BF} at low doping is lower than at high doping. As the applied potential further increases, the electrons that enter the p_1 layer and are not recombined will pass through the p_1 layer and reach Jn_2/p_1 under the action of the electric field. Because Jn_2/p_1 is reverse biased at this time, a large number of electron–hole pairs will be generated at this junction due to the avalanche multiplication or tunneling mechanism. Jn_2/p_1 will then be broken down and cause the LED to enter the conduction region (that is, the ON-state), as shown in figure 3(c). According to figure 2, when Jn_2/p_1 is broken down, the *I–V* characteristics of the LED will present an NDR, and the forward voltage (V_{f}) at this time will drop rapidly. It can also be found that the rate of current rise is faster for low doping flow rates in the NDR range than for high doping flow rates. This may be because when the Mg doping concentration of the p_1 layer is lower, the probability of electrons being captured and recombined by holes will be reduced, and the n_1 layer has a very high electron concentration. It is thus assumed that the p_1 layer has the same electron injection efficiency at high or low doping flow rates. Compared with high Mg doping flow rates, more electrons are injected into the n_2 layer under low doping flow rates, causing the current located in the NDR region to rise rapidly, as shown in figure 2.

For the shift of the *I–V* characteristics, we take figure 2(b) as an example to illustrate possible changes. When the Mg doping flow rate increases from 0.036 to 0.255 μmol min^{-1}, as shown in figure 3(b), the barrier height at Jp_1/n_1 will rise, which will cause the V_{BF} to increase accordingly. And due to the increase in the hole concentration, the probability of electrons entering the p_1 layer being captured and recombined by holes also begins to increase. As a result, the resistance of the LED will increase when there is a lack of freely mobile carriers in the p_1 layer, resulting in an increase in V_{f} in the forward conducting region. Based on the above reasons, it can be found from figure 2(b) that the *I–V* characteristics shift to the right. Further increasing the Mg doping flow rate from 0.255 to 1.057 μmol min^{-1}, it can be seen from figure 2(b) that V_{h} decreases with the increase of the doping flow rate at the same current. Taking Si- or GaAs-based abrupt *p–n* junction diodes as an example, their breakdown voltage will decrease with the increase of doping concentration. As shown in figure 3(d), increasing the doping concentration of the p_1 layer will increase the barrier height difference at Jn_2/p_1,

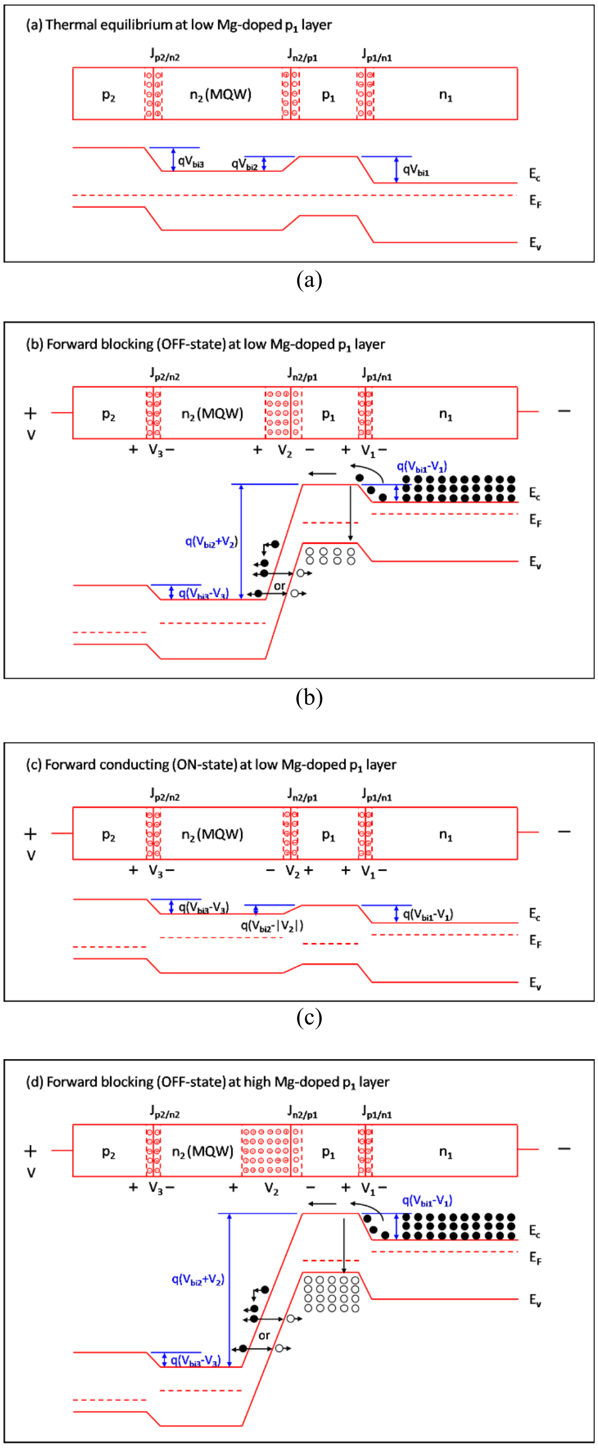

Figure 3. Energy-band diagrams of thyristor-like InGaN-based LEDs at thermal equilibrium, forward blocking, and forward conducting. (a)–(c) are low Mg-doped p_1 layer, and (d) is high Mg-doped p_1 layer. The energy-band diagrams of the high Mg-doped p_1 layer at thermal equilibrium and forward conducting are similar to those of the low Mg-doped p_1 layer. The difference is that the barrier height of Jp_1/n_1 is different. Therefore, it is not shown here.

compared with figure 3(b). Because the barrier height difference at Jn_2/p_1 becomes larger, more carriers will be generated by avalanche multiplication or tunneling mechanism, resulting in the easy breakdown of Jn_2/p_1. So, it can be found from figure 2(b) that V_h with higher doping concentration drops rapidly compared with lower doping concentration, and the *I*–*V* characteristics also shift to the left at the same time. Finally, at a very high Mg doping flow rate (1.349 μmol min^{-1}), most of the electrons are captured by the holes in the p_1 layer, so the lack of free carriers in this layer leads to an increase in the series resistance (R_s). At this time, compared with the Mg doping flow rate of 0.583–1.057 μmol min^{-1}, it can be found that V_f increases rapidly at the same current, and therefore, the *I*–*V* characteristics in figure 2(b) shift to the right again. Since the number of electrons entering the MQW is significantly reduced, it can be found that the LED hardly emits light during *I*–*V* testing.

Figure 4 shows the variation of the *I*–*V* characteristics of thyristor-like InGaN-based LEDs at various thicknesses when the Mg doping flow rate is the same. It can be found that, in addition to V_{BF}, the voltage of the forward conduction region also increases with thickness. This may be because when the thickness of the p_1 layer increases, the probability of electrons passing through the p_1 layer being captured and recombined increases, resulting in a decrease in the concentration of free carriers in this layer, which increases the resistance of the p_1 layer. Therefore, comparing figures 2 and 4 shows that the *I*–*V* characteristic with NDR has a smoother curve and no two NDR regions appear when the Mg doping flow rate is 0.583–1.057 μmol min^{-1} and the thickness is 300–400 nm. In other words, under these parameter settings, the thyristor-like InGaN-based LED has an *I*–*V* characteristic similar to that of a thyristor.

There is, however, a peculiar phenomenon in the variation of the thickness versus *I*–*V* characteristics, as shown in figure 5. To concisely show those *I*–*V* characteristics with two NDR regions, we have removed the curves for the 900 nm-thick p_1 layer that could cause damage to the LEDs. Figure 5 shows the change of the *I*–*V* characteristics as the thickness increases when the Mg doping flow rate is lower than 0.401 μmol min^{-1}. It can be seen that the *I*–*V* characteristics with two NDR regions become more and more obvious with the increase of thickness. And when the thickness is the same, the *I*–*V* characteristics with two NDR regions will become more apparent as the Mg doping flow rate reduces. Moreover, when the Mg doping flow rate is 0.255 μmol min^{-1}, the *I*–*V* characteristics with two NDR regions only appear in the structure with a p_1 layer thickness higher than 300 nm, while the *I*–*V* characteristics do not appear as two NDR regions when the thickness is 300 nm or below. Both cases seem to indicate that the formation of two NDR regions on the *I*–*V* characteristics is related to the insufficient conductivity of the p_1 layer.

Figure 6 illustrates the possible causes for the formation of two NDR regions on the *I*–*V* characteristics by taking the

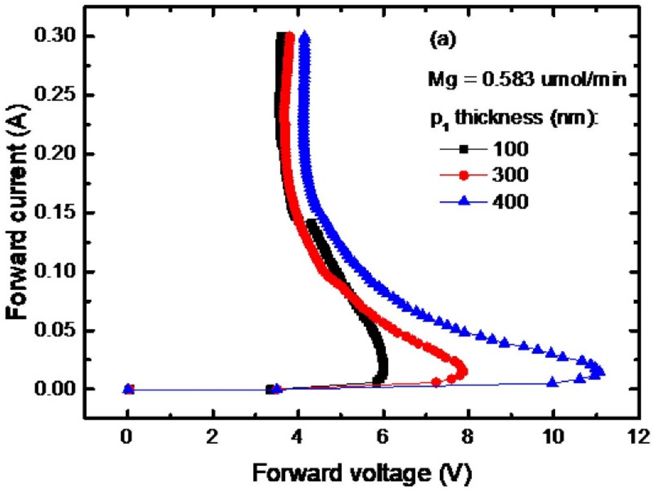

(a)

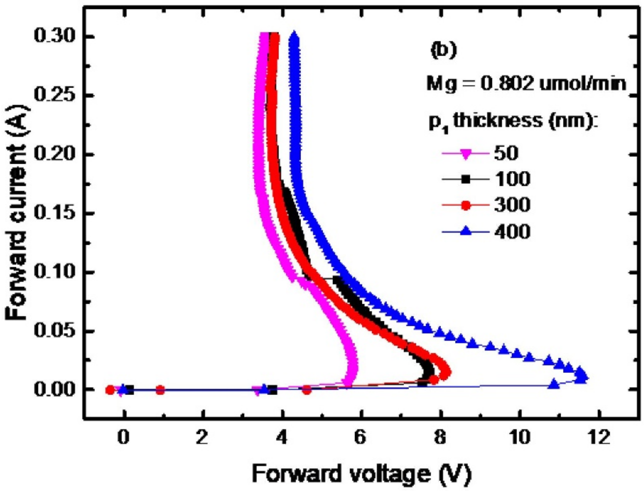

(b)

Figure 4. *I–V* characteristics of the thyristor-like InGaN-based LEDs with different p_1 layer thicknesses when the Mg doping flow rates are 0.583 and 0.802 μmol min^{-1}, respectively.

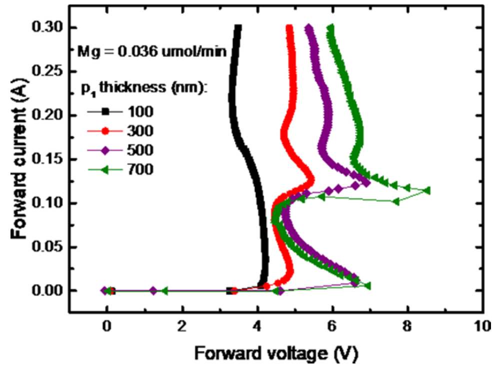

Figure 5. The *I–V* characteristics of thyristor-like InGaN-based LEDs show two NDR regions.

Mg doping flow rate of 0.036 μmol min^{-1} and the thickness of 300 nm as an example. The energy-band diagrams in figures 6(b)–(d) correspond to the three regions on the *I–V* characteristics in figure 6(a). When a small positive potential is applied to the LED, after the electrons gain enough energy to cross the barrier at Jp_1/n_1 and enter the p_1 layer, the V_{BF} will form in the *I–V* characteristics. Due to the low Mg doping flow rate ($\leqslant$0.255 μmol min^{-1}) in the p_1 layer, the probability of electrons from the n_1 layer being captured by holes is relatively low. Therefore, these electrons that are not captured by the holes will reach Jn_2/p_1 under the action of the electric field. The current at this time will rise rapidly due to the breakdown of Jn_2/p_1 and form the first NDR on the *I–V* characteristics, as shown in Region I of figure 6(a). However, it can be found from Region II of figure 6(a) that when the applied current further increases, the voltage drop on the LED does not decrease but increases instead. Even the second V_{BF} (at high current) is higher than the first one (at low current). It, therefore, is inferred that Jn_2/p_1 may remain reverse biased and has not yet breakdown. As can be seen from the voltage applied to the thyristor-like LEDs structure in figure 3(b), the voltage across the device is the sum of the voltage drops across the three junctions (Jp_1/n_1–Jp_2/n_2), that is, the voltage drop in the OFF-state is given by $V = V_1 + V_2 + V_3$. And in the ON-state, the voltage drop of the LED is $V = V_1 + |V_2| + V_3$, such as figure 3(c). Hence, the voltage in the OFF-state should be higher than that in the ON-state. It can be found from figure 6(a) that the voltage in Region II rises again as the current increases. Until the higher applied current, it can be found that the *I–V* characteristics appear as a second NDR, as shown in Region III of figure 6(a). Finally, the LED enters the forward conducting region because Jn_2/p_1 is broken down. As a result, we speculate that $\mathrm{Jn_2/p_1}$ is still reverse-biased. The reason for this may be as follows.

We can use the change of the carrier concentration to illustrate its influence on the conductivity of the p_1 layer. The conductivity of the p_1 layer is given by

$$\sigma = \frac{1}{\rho} = q\left(\mu_n n + \mu_p p\right) \tag{1}$$

where n and p are the concentrations of electrons and holes in the $\mathrm{p_1}$ layer, respectively. Since the p_1 layer is a p-type semiconductor, its resistivity can be simplified to the following expression:

$$\rho_p = \frac{1}{q\mu_p p} \tag{2}$$

where μ_p is the mobility of the hole. Although the hole concentration of the p_1 layer is not high under low Mg doping ($\leqslant$0.255 μmol min^{-1}), the electron concentration injected into the p_1 layer may also not be high in the low applied current range, as shown in figure 6(b). At this time, the ratio of the

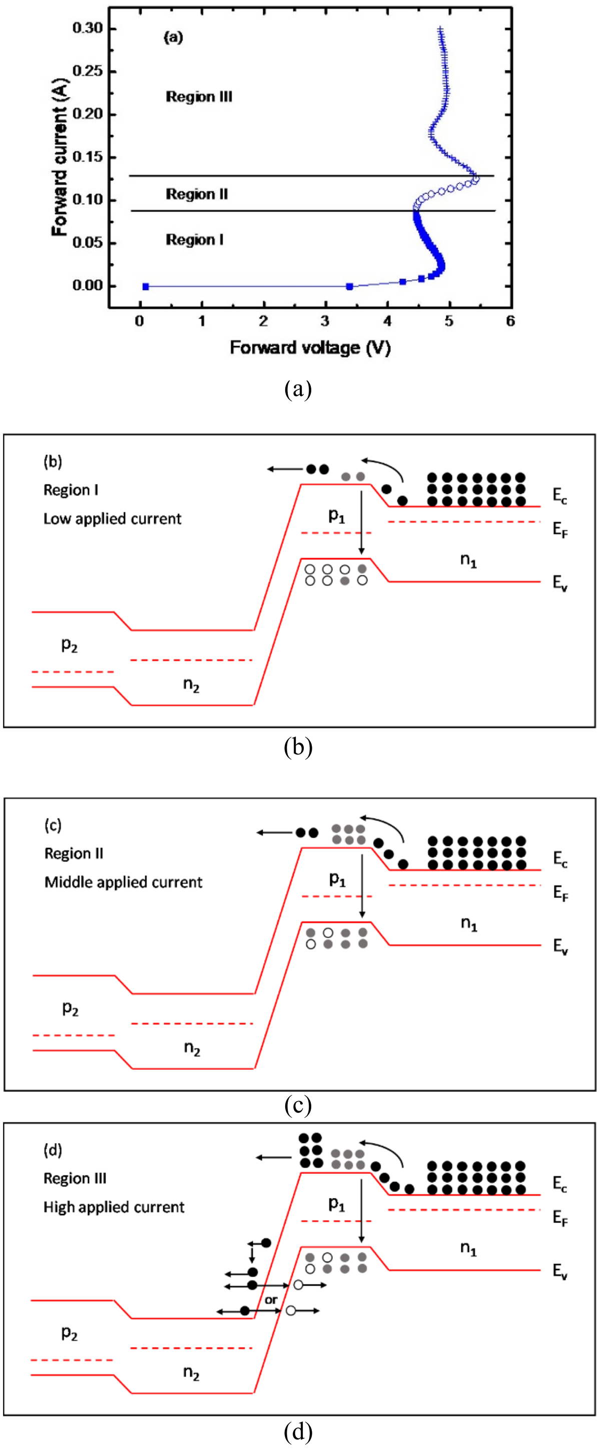

Figure 6. Possible causes for the formation of two NDR regions. (a) *I–V* characteristics of the thyristor-like InGaN-based LEDs with an Mg doping flow rate of 0.036 μmol min^{-1} and a thickness of 300 nm. (b)–(d) are the conduction of carriers in the p_1 layer at low, medium, and high applied currents, respectively. The black dots represent electrons, the white dots represent holes, and the gray dots represent recombined electron–hole pairs.

holes occupied by electrons to the overall hole concentration may not be high. It can be seen from Equation 2 that the p_1 layer still has a certain concentration of holes that can help electrons transport, so the influence on the resistivity of the p_1 layer is limited. Hence, it can be found from figure 6(b) that once the electrons cross the barrier at Jp_1/n_1 and reach the p_1 layer, a V_{BF} is formed. These electrons that are not captured by the holes then enter the n_2 layer and create the first NDR. As the applied current increases, more electrons should be injected into the p_1 layer, and the probability of these electrons being captured by holes also increases, as shown in figure 6(c). Therefore, the ratio of holes occupied by electrons to the overall hole concentration increases. It can be known from Eq. 2 that the decrease in the free hole concentration will lead to an increase in the resistivity of the p1 layer, and the voltage will rise again as the current increases. Until a higher current is applied, as shown in Region III of figure 6(a), more electrons will be injected into the p_1 layer and reach Jn_2/p_1 under the action of a high electric field. Although the free hole concentration of the p_1 layer may be reduced due to the injection of electrons, under the action of a high electric field, electrons may still reach Jn_2/p_1 with the help of free holes. Then, they will cause Jn_2/p_1 to break down due to avalanche multiplication or tunneling mechanisms and form a second NDR on the *I–V* characteristics, as shown in figure 6(d). As a result, we speculate that the appearance of the two NDR regions is related to the insufficient conductivity of the p_1 layer. Hence, comparing figures 2, 4, and 5, it can be found that the optimal conditions for forming a thyristor-like InGaN-based LED are an Mg doping flow rate of 0.583–1.057 μmol min^{-1} and thickness of 300–400 nm.

Figure 7 shows the brightness change at different Mg doping flow rates or thicknesses. It should be pointed out that the Advantest R6243 source meter uses manual mode for optical output power testing, not the automatic method like the Keithley 2400 for *I–V* testing. Therefore, the test results in figure 7 may have variations compared with figure 2. Figure 7(a) is the *L–I–V* curves of the p_1 layer with a thickness of 300 nm at different Mg doping flow rates. The trends of their *I–V* characteristics are similar to those in figure 2(b). When the applied current is greater than 150 mA, the Mg doping flow rate of 1.349 μmol min^{-1} will have a higher voltage than other lower Mg doping flow rates. However, the optical output power will attenuate as the Mg doping flow rate increases. Figure 7(b) is the *L–I–V* curves when the p_1 layer has different thicknesses under the Mg doping flow rate of 0.802 μmol min^{-1}. It can be found that as the thickness increases, the voltage will rise while the optical output power will decrease. It can be seen from figure 7(a) that if the thickness is 300 nm, when the Mg doping flow rates are 0.583, 0.802, and 1.057 μmol min^{-1}, the optical output powers of the thyristor-like InGaN-based LED are 13.1, 12.8, and 14.3 mW at a current of 201 mA, respectively. And at the current of 4.61 mA, the optical output powers are 0.46, 0.52, and

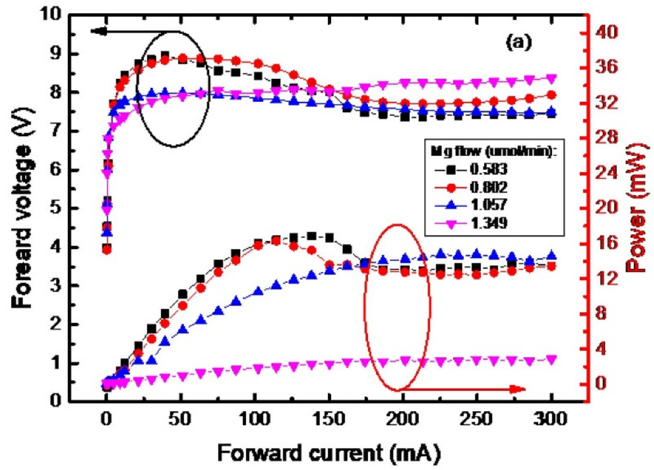

(a)

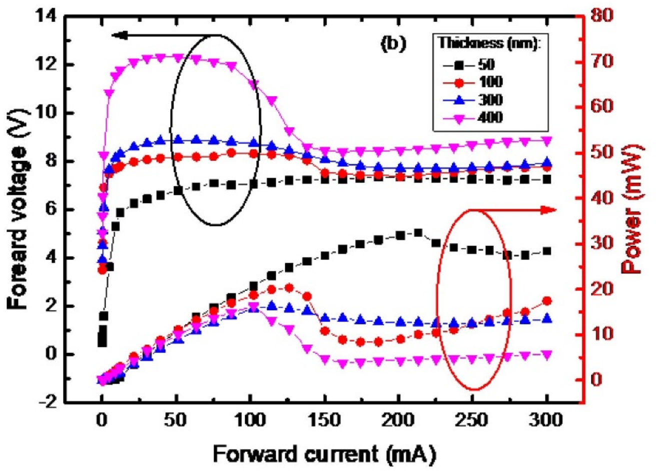

(b)

Figure 7. *L–I–V* curves of the thyristor-like InGaN-based LEDs. (a) *L–I–V* curves of different Mg doping flow rates at a p1 layer thickness of 300 nm, and (b) *L–I–V* curves of different *p*1 layer thicknesses at an Mg doping flow rate of 0.802 μmol min^{-1}.

0.54 mW, respectively. There is a 24-fold difference in brightness between light and dark, which should help distinguish whether the light is on or off. The output power decreases monotonously with the increase of Mg doping flow rate or thickness, as shown in figures 7(a) and (b). This should mean that the probability of electrons being captured and recombined by holes will increase as the Mg doping flow rate and thickness increase when the electrons from the n_1 layer pass through the p_1 layer, so that the electrons injected into the n_2 layer are significantly reduced. Even though reducing the thickness of the p_1 layer helps to improve the output power, it will bring another problem for the thyristor-like LEDs fabricated as a three-terminal device. One is for the *n*-electrode, another is for the *p*-electrode, and the other is for the gate electrode. A positive potential (V_g) is usually applied to the p_1 layer to change the voltage of the V_{BF} to speed up the switching speed of the Si-based thyristor. Part of the p_1 layer will be etched, and a gate electrode will be made on the exposed p_1 layer. Therefore, the thyristor-like InGaN-based LEDs need to undergo two inductively coupled plasma (ICP) etchings when it is fabricated into a three-terminal device. To precisely control the depth of ICP etching, the thickness of the p_1 layer will become critical.

It can also be found from figures 7(a) and (b) that when NDR appears in the *I–V* characteristics, the optical output power will have an obvious attenuation at the corresponding position. This may be as shown in figure 3(c), when Jn_2/p_1 enters the forward conducting region due to the avalanche or tunneling breakdown, the E_F of n_2 moves upward. The probability of electrons from the n_1 layer occupying an energy level above the conduction band (E_c) of the n_2 layer becomes smaller. The reduction of electrons injected into the quantum well will further affect the luminous efficiency of the MQW. Comparing figures 3(b) or (d) and 7, it can be found that before the NDR is completely formed, a large number of electrons which derives from the avalanche multiplication or tunneling mechanism are injected into the n_2 layer, and the output power increases with the increase of the current, as shown in figures 7(a) and (b). Once the LED enters the forward conducting region as shown in figure 3(c), since the E_F of n_2 moves up and affects the number of electrons injected into the MQW, the output power will decline after the NDR is fully formed, as shown in figures 7(a) and (b). More research on this phenomenon may be needed. Besides, the forward voltages at 201 mA for three different Mg doping flow rates are 3.71, 3.75, and 3.95 V, respectively. It can be found from figure 2 or 4 that the holding current (I_h) when V_h occurs is relatively high. The current in the subsequent forward conducting region is also relatively high. Too higher an operating current will greatly hinder the application of thyristor-like LEDs. High operating current not only makes the LEDs hot but also is not conducive to energy saving. Therefore, it is necessary to adjust and optimize the structure of the thyristor-like LEDs to improve the luminous efficiency. In this way, the thyristor-like LEDs will have both the function of a switch and the ability to emit light to expand more applications.

4. Conclusion

The thyristor is a bistable device that possesses high impedance, low current in the OFF-state, and low impedance, high current in the ON-state. By combining this distinctive bistable characteristic, we can switch the LED from the OFF-state, which emits no light, to the ON-state, which emits light, via a proper applying voltage. To achieve this purpose, an extra *p*-GaN layer is introduced into the InGaN-based LEDs structure between the *n*-GaN and MQW. Using the thyristor-like structure, we can find that an NDR appears on the *I–V* characteristics of InGaN-based LEDs. The formation of NDR is mainly affected by the Mg doping concentration and thickness of the additionally added *p*-GaN layer. In our structure, the Mg doping flow rate of about 0.583–1.057 μmol min^{-1} and the thickness of about 300–400 nm have the best NDR properties. When the thickness is 300 nm, and the Mg doping flow rates are 0.583, 0.802, and 1.057 μmol min^{-1}, the optical output powers of thyristor-like InGaN-based LEDs at the current of 201 mA are 13.1, 12.8, and 14.3 mW, respectively. While at the current of 4.61 mA, the output powers are 0.46, 0.52, and 0.54 mW. This brightness difference of more than 24 times should help to distinguish the light on and off. In addition, the forward voltages at 201 mA are 3.71, 3.75, and 3.95 V for the Mg doping flow rates of 0.583, 0.802, and 1.057 μmol min^{-1}, respectively. However, the holding current is still high, resulting in a high operating current when the thyristor-like LEDs are turned on. Therefore, the structure of the thyristor-like LEDs needs to be further adjusted and optimized to reduce the operating current.

Data availability statement

All data that support the findings of this study are included within the article (and any supplementary files).

Acknowledgments

The authors acknowledge support from Singapore Agency for Science, Technology, and Research (A*STAR) MTC program, Grant No. M21J9b0085. This research is supported by the Ministry of Education, Singapore, under its Academic Research Fund Tier 1 (MOE-RG62/20).

The authors would also like to thank Professor Wen Ray Chen, Department of Electronic Engineering, National Formosa University, Yunlin, Taiwan, for providing the *I–V* test equipment and valuable comments. We would also like to thank the Lighting engine development Laboratory for their assistance in *I–V* testing.

ORCID iDs

Ping Chieh Tsai https://orcid.org/0009-0003-9332-8119
Chunyu Zhao https://orcid.org/0000-0001-6643-343X
Swee Tiam Tan https://orcid.org/0000-0002-2046-0309
Hilmi Volkan Demir https://orcid.org/0000-0003-1793-112X

References

[1] Matsuoka T, Okamoto H, Nakao M, Harima H and Kurimoto E 2002 *Appl. Phys. Lett.* **81** 1246
[2] Mukai T, Yamada M and Nakamura S 1999 *Proc. SPIE* **3621** 2–13
[3] Funato M, Ueda M, Kawakami Y, Narukawa Y, Kosugi T, Takahashi M and Mukai T 2006 *J. Phys. D: Appl. Phys.* **45** L659
[4] Bezshlyakh D D, Spende H, Weimann T, Hinze P, Bornemann S, Gülink J, Canals J, Prades J D, Dieguez A and Waag A 2020 *Microsyst. Nanoeng.* **6** 1
[5] Hun C J, Lee S J, Kwon K O, Choi J Y, Jung T, Han M and Han S J 2020 *Appl. Phys. Express* **13** 026501–1
[6] Haas H, Yin L, Wang Y and Chen C 2016 *J. Lightwave Technol.* **34** 1533
[7] Matsuda K, Takimoto K, Lee D-H and Shibata J 1990 *IEEE Trans. Electron Devices* **37** 1630
[8] Numai T, Sugimoto M, Ogura I, Kosaka H and Kasahara K 1991 *Appl. Phys. Lett.* **58** 1250
[9] Taylor G W, Simmons J G, Cho A Y and Mand R S 1986 *J. Appl. Phys.* **59** 596
[10] Choi W-K, Kim D-G, Moon Y-T, Choi Y-W, Kim Y-K, Choquette K D, Lee S and Woo D-H 2006 *Appl. Phys. Lett.* **89** 121117–1
[11] Sze S M and Kwok K N 2006 *Physics of Semiconductor Devices* 3rd edn (Wiley)
[12] Stringfellow G B 1989 *Organometallic Vapor Phase Epitaxy: Theory and Practice* 1st edn (Academic Press)